J Mater Sci (2011) 46:5090–5096
DOI 10.1007/s10853-011-5438-3

Microstructural evolution during creep of a hot extruded 2D70Al-alloy

Guo-jun Wang · Bai-qing Xiong · Yong-an Zhang

Received: 17 January 2011 / Accepted: 2 March 2011 / Published online: 12 March 2011

Abstract Microstructural evolution during creep of a hot extruded Al–Cu–Mg–Fe–Ni (2D70) Al-alloy was investigated in this study using transmission electron microscopy (TEM). The samples for creep test were carried out two-stage homogenization, followed by extruding. The creep ultimate strength dropped and the temperature increased gradually from 312 to 117 MPa and from 423 to 513 K, respectively. The microstructural observation for the crept samples showed that the S′ phase coarsened with increased creep temperature and the aging precipitates transformed from S″ phase to S′ phase during creep process. Meanwhile, excess solute atoms in supersaturated solid solution dynamically precipitated to further form finer S′ phase and S″ phase, which pinned the dislocations and impeded the dislocation movements. Large amount of dislocations piled up around the micron-scale Al_9FeNi phase, and a lot of dislocation walls were generated along ⟨220⟩ orientation. S phase accumulates around these defects. The interaction between dislocations and precipitates was beneficial for the improved performances at elevated temperature.

Introduction

The 2D70 aluminum alloy is an Al–Cu–Mg alloy with Fe and Si additions to form intermetallic phases. This alloy is designed for parts operating at elevated temperatures which are manufactured not only by forging but also by extrusion and rolling. Heavily loaded engine pistons, parts of aircraft engines, cladding of ultrasonic aircrafts (e.g., Concorde), etc. operating in a long-term at temperature up to 150 °C are manufactured from this alloy [1]. Compared to other 2XXX series alloys, Al–Cu–Mg–Fe–Ni series alloys have good elevated temperature strength [2]. The effects of deformation aging treatment on the microstructure and properties of 2618 alloy, which has similar chemical compositions with 2D70 alloy but has relatively higher impurities content, were investigated [3–5]. The effect of trace elements additions, such as Ti, Sn, and Y, on fine Al_9Ni phase formation and their mechanical properties were studied [4]. Yu et al. analyzed the mechanical properties and microstructures of aluminum alloy 2618 containing scandium and zirconium, showing that adding scandium and zirconium elements to 2618 alloy resulted in a primary $Al_3(Sc,Zr)$ phase, and that the strength increased at both ambient and elevated temperatures without a decrease of ductility [6].

However, only a few of them have tried to relate the evolution of the hardening precipitation during creep with creep behaviors [7]. Roldan and Sifferlent showed that at 125 °C the coarsening of the S′ hardening precipitates took place during the tertiary stage of creep, leading to a change in the creep mechanism [8], and this was confirmed by Singer and Blum [9]. Novy et al. investigated the microstructure changes in a 2618 aluminum alloy during aging and creep at 270 °C at a constant load of 140 MPa, and showed that fine and coherent precipitates of S-phase distributed dispersively in the matrix of the alloy after aging to peak condition and coarsened at elevated temperature during the creep test, and that numerous partially coherent needle-like S-precipitates were formed [1]

G. Wang (✉)
Northeast Light Alloy Co., Ltd., Harbin 150060, China
e-mail: wangguojundq@126.com

G. Wang · B. Xiong · Y. Zhang
State Key Laboratory for Fabrication and Processing of Nonferrous Metals, General Research Institute for Nonferrous Metals, Beijing 100088, China

The microstructure of an as-cast Al–Cu–Mg–Fe–Ni aluminum alloy and its microstructural evolution during homogenization were investigated in the previous study, indicating that, under double homogenization, the high melting point Al/Al_2Cu phases were dissolved, and no obvious change was observed regarding the size and morphology of Al_9FeNi, Cu_2FeAl_7, and Al_7Cu_4Ni compounds [10]. In the present investigation, microstructural evolution of a double-homogenizied 2D70(Al–Cu–Mg–Fe–Ni) alloy crept at temperature up to 513 K was studied in detail.

Experimental procedure

The as-received Al–Cu–Mg–Fe–Ni alloy ingot prepared by continuous casting with an approximate chemical composition of 0.16%Si, 1.26%Fe, 2.33%Cu, 1.7%Mg, 0.1%Cr, and 1.24%Ni with the balance as Al (all in wt%) was used in this study. The cast billets were first double-stage homogenized, which involved solution treatment at 763 K for 16 h and then at 803 K for 16 h, followed by cooling in the furnace. The solution-treated billets were forged, and then extruded with a reduction rate of 12.3 at 803 K to rods with diameter of 85 mm. Before the extrusion processing, the billets were held in a furnace at 803 K for 2 h. After extrusion, the samples were solution treated at 808 K for 1 h and aging treated at 468 K for 20 h. The aged rods were machined into creep test pieces of 10 mm in diameter and 100 in gauge length. Creep experiments were carried out under a constant nominal stress at 423, 453, 483, and 513 K, respectively for 100 h for all the samples to produce a maximum strain of 0.2% according to the standard of GB/T2039-1997. The crept microstructures were observed using JEM-2000FX transmission electron microscope (TEM) operating at 200 kV. For TEM analysis, disks with 3 mm in diameter were cut from the as-extruded ingots and ground to a thickness of 0.07 mm. The thin foils for TEM observation were electrolytically polished in the solution of 33% HNO_3 with methanol. Before observation, the foils were cleaned by Gatan 691 device using low energy Ar particle beam at 253 K.

Results and discussion

Microstructures of aged 2D70 alloy

The TEM images and corresponding selected area electron diffraction patterns (SAED) of peak-aged alloy are shown in Fig. 1. The main precipitates are S′ phase and S phase. The S phase is rod shaped or lath shaped, which generally precipitates in habit plane at the matrix of {021} and prolongs at ⟨100⟩ direction. The strip-shaped S′ phase with a weaker contrast and an average length of 50 nm precipitates mainly along [001] and [010] directions. The irregular particles are the S phase precipitates at {021} crystal planes, in which the section of precipitated particles is observed in this direction actually.

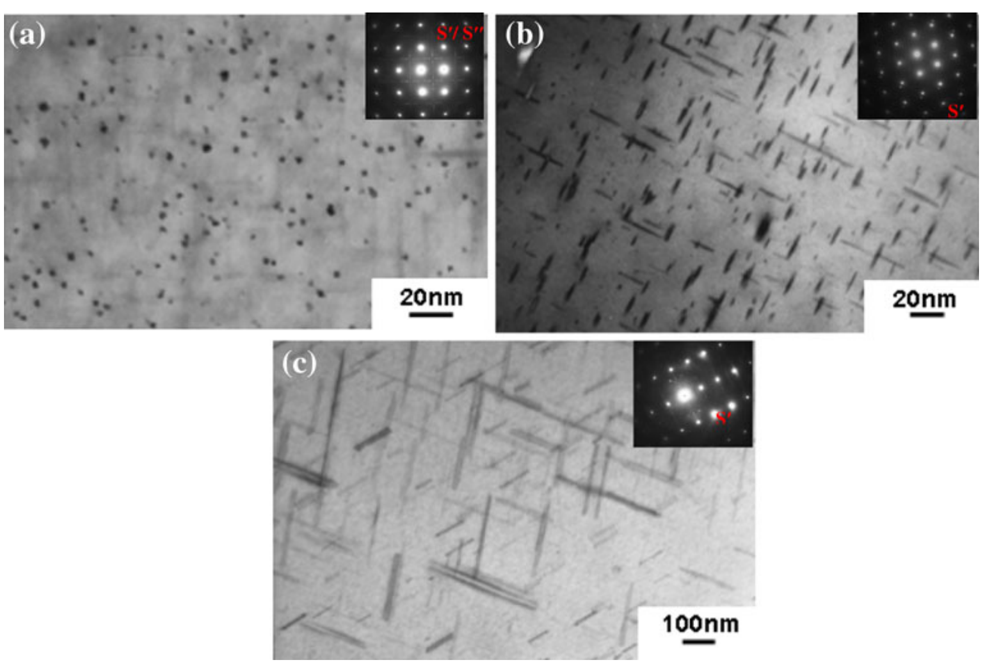

Fig. 1 TEM micrographs and corresponding diffraction patterns of the aged 2D70 alloy in: **a** [100] zone, **b** [110] zone, and **c** [112] zone

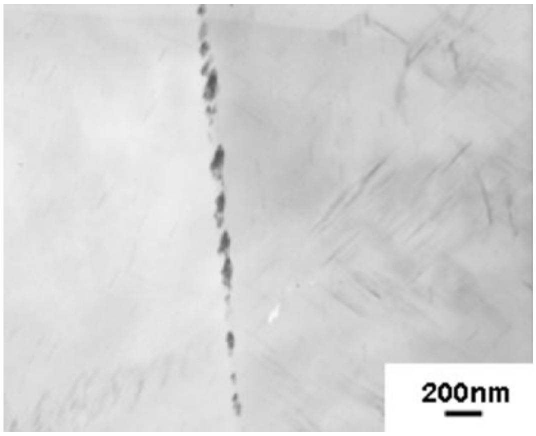

Fig. 2 Precipitates at large-angle grain boundary

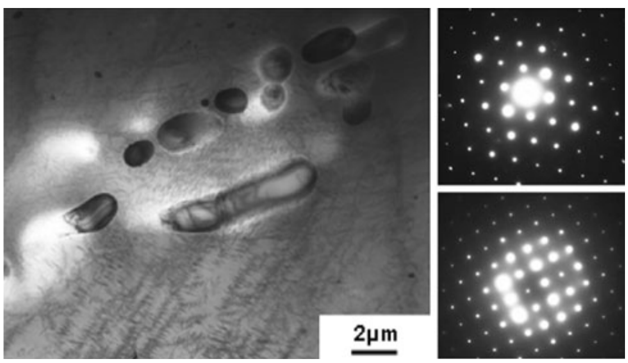

Fig. 3 TEM micrographs and corresponding diffraction pattern of Al_9FeNi phase within grain

Figure 2 shows the discontinuous precipitates at large-angle grain boundary. Al_9FeNi phase is distributed within grain, and the corresponding SAED patterns are shown in Fig. 3. Figure 4 shows the relationship between the creep ultimate strength and tested temperature. The creep temperature has a significant effect on creep ultimate strength. The creep ultimate strength decreases from 312 MPa at 150 °C to 117 MPa at 240 °C.

Microstructural analysis during creep

Microstructures of 2D70 alloy crept at 150 °C

Figure 5 shows TEM bright field (BF) images and SAED patterns of 2D70 alloy crept at 150 °C for 100 h. The diffraction spots of S″ are observed in the diffraction pattern along zone axis [100], which are not found in the aged sample before creep. Eight diffraction spots with various included angles are distributed around central diffraction spot, caused by S phase precipitated at the family of {021} crystal planes, as shown in Fig. 5a. The precipitated S phase at aging treatment coarsens to an average size of

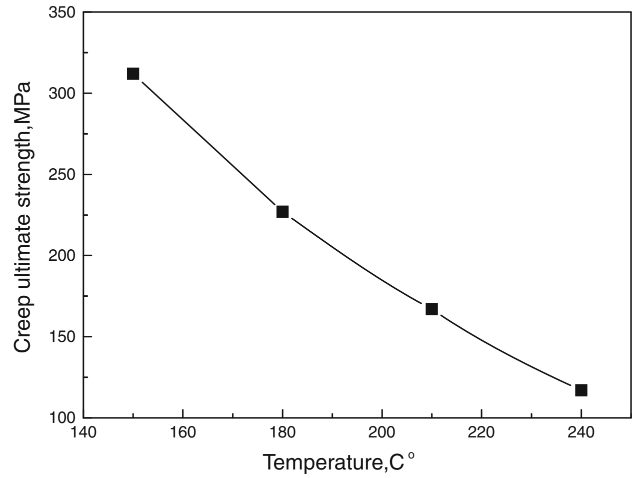

Fig. 4 Creep ultimate strength of the 2D70 alloy as a function of test temperature

350 nm observed in [100] direction as shown in Fig. 5a. Figure 5b and c shows respectively the TEM BF images and SAED pattern observed along [112] and [110], in which needle-like precipitates in nanometer scale occur and are confirmed to be S phase.

Figure 6 shows the morphology along [100] zone axis, showing a great number of wave-shaped contrasts at [022]. These are the dislocations yielded during creep. S phase congregates in the slide plane with a lot of defects, impeding dislocation movement, and resulting in an increased creep resistance.

The S phase precipitated on the dislocation is given in Fig. 7a, and interaction between precipitates and dislocations is shown in Fig. 7b, showing the obvious pinning of precipitates to dislocations. There is a small quantity of S phases.

There are discontinuous precipitates distributed at large-angle boundaries as shown in Fig. 8a, and a lot of dislocations are stacked around Al_9FeNi phase in nanometer scale as shown in Fig. 8b.

Microstructures of 2D70 alloy crept at 180 °C

The BF images and SAED patterns for sample crept at 180 °C for 100 h along [100], [110] and [112] zone axis are given in Fig. 9. The diffraction spots of S″ phase are obtained apart from those of S phase, indicating that the two precipitated phases, S and S″, are formed after creep at 180 °C. S phase precipitates during aging treatment and coarsens to 360 nm as shown in Fig. 9b. Fine phase S precipitates are dynamically formed during creep as shown in Fig. 9c as observed from the BF images along [100] zone axis.

There are discontinuous precipitates distributing at large-angle boundaries as shown in Fig. 10a. S phase

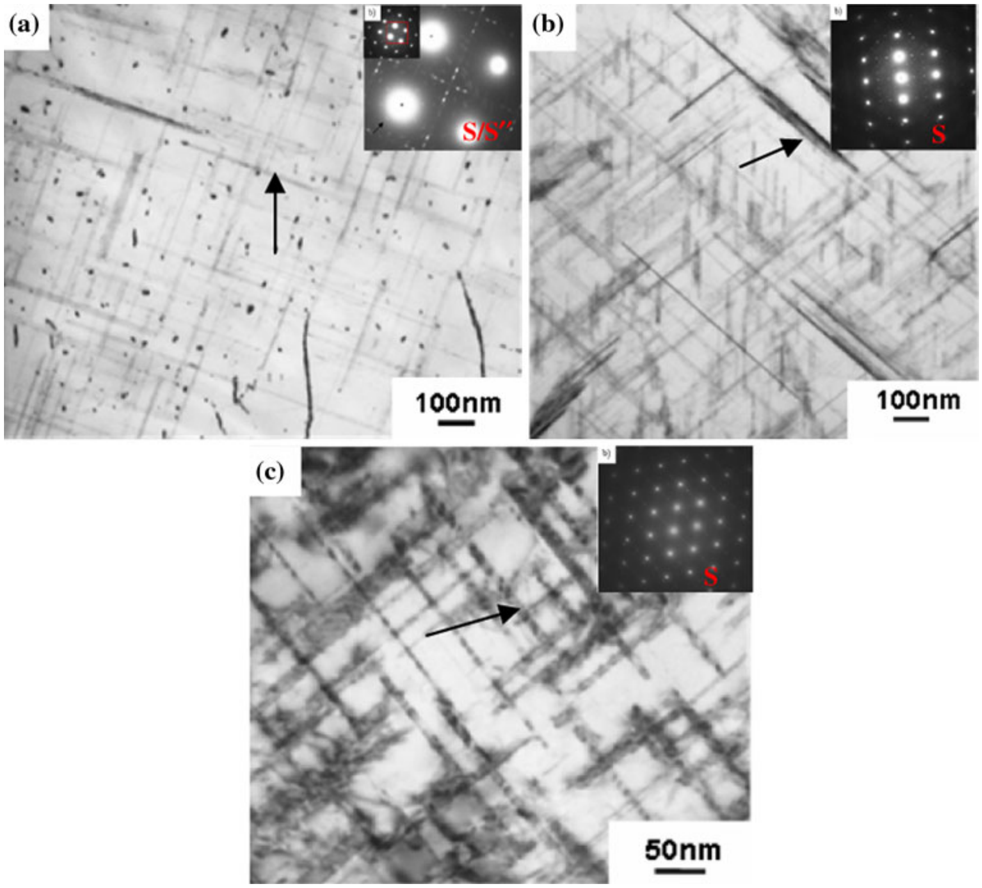

Fig. 5 TEM micrographs and SAED pattern zone after creep at 150 °C for 100 h in: **a** [100] zone, **b** [112] zone, and **c** [110] zone

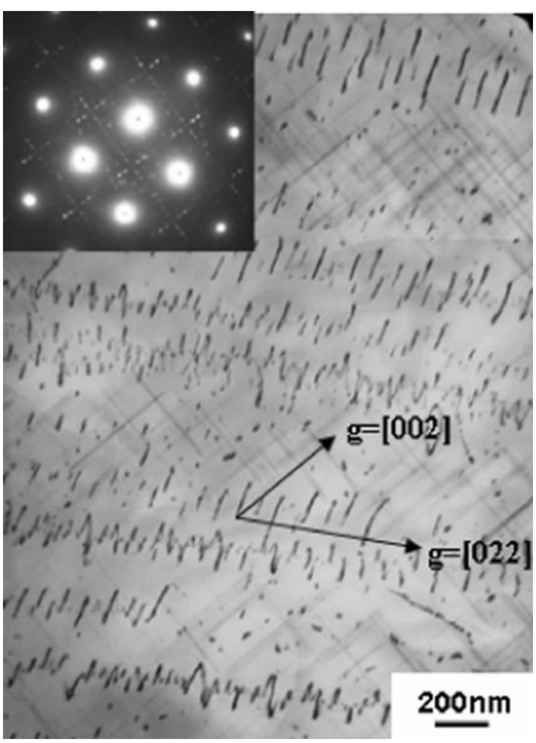

Fig. 6 Precipitated S phase distributed along ⟨022⟩ direction

enriched near the dislocation is observed in Fig. 10b. The stress contrast and dislocation distribution are shown in Fig. 11.

Microstructures of 2D70 alloy crept at 240 °C

The microstructures of 2D70 alloy crept at 240 °C for 100 h are shown in Fig. 12. The S phase precipitated during aging treatment is coarsened to an average length of 480 nm. Meanwhile, a small quantity of fine particles is precipitated dynamically at grain boundary, as shown in Fig. 13a, and the interaction between precipitates and dislocations is shown in Fig. 13b.

The creep behavior of aluminum alloys can be described by the following equation [11]:

$$\bar{\varepsilon} = \frac{2\rho_m \Phi_p (1 - \Phi_p)\left[\sqrt{\frac{\pi}{4\Phi_p}} - 1\right] c_j D_m}{M} \sinh\left(\frac{\sigma_{eff} b^2 \lambda}{\alpha MKT}\right)$$

where $\bar{\varepsilon}$ is the main creep rate, ρ_m is the flow dislocation density, φ_p is the particle volume fraction, c_j is the dislocation jog density, D_m is the diffusion coefficient of the matrix, M is the Taylor factor, α is the uniform sequence

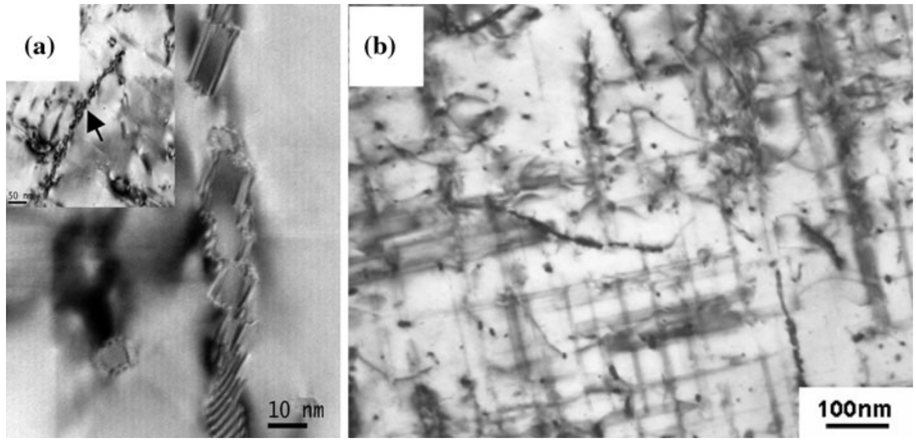

Fig. 7 Interaction of S phase and dislocations: **a** HERM micrographs of S phase precipitated on the dislocations and **b** S phase and dislocations

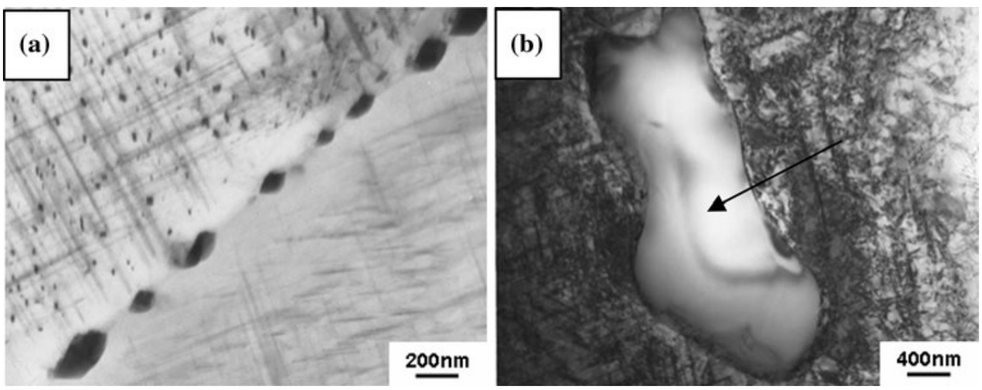

Fig. 8 Discontinuous S phase on grain boundary (**a**) and dislocation distribution around Al_9FeNi particle (**b**)

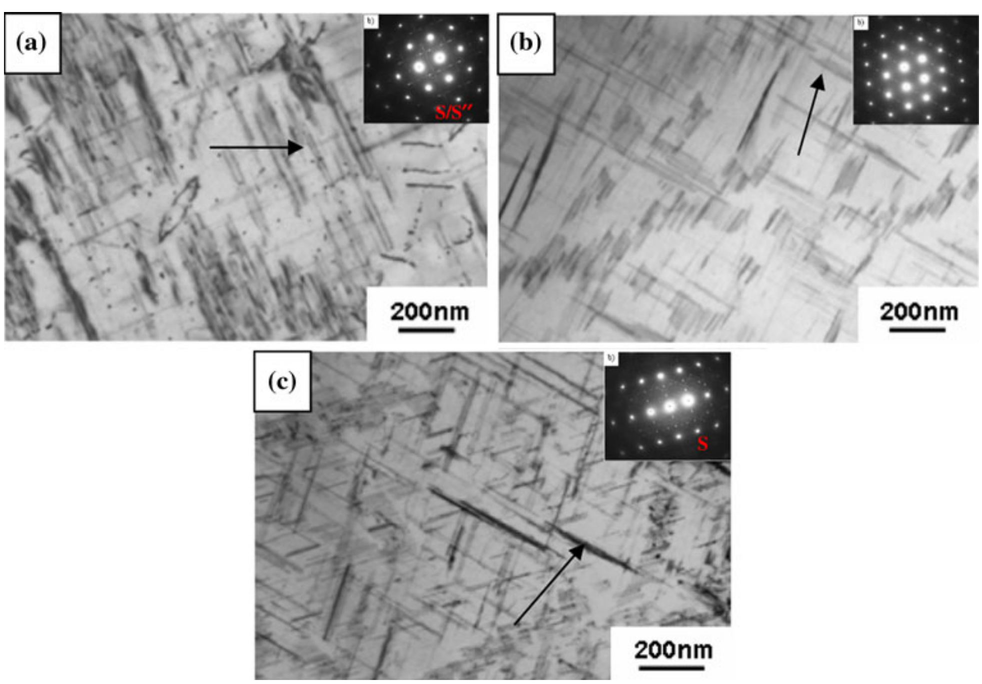

Fig. 9 TEM micrographs and SAED pattern of 2D70 alloy crept at 180 °C for 100 h in: **a** [100] zone, **b** [112] zone, and **c** [110] zone

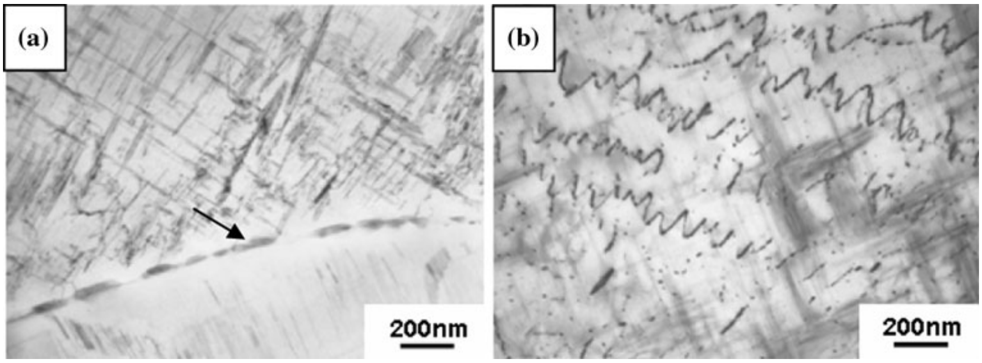

Fig. 10 Discontinuous precipitations on large-angle grain boundary (**a**) and enriched S phases around dislocation (**b**)

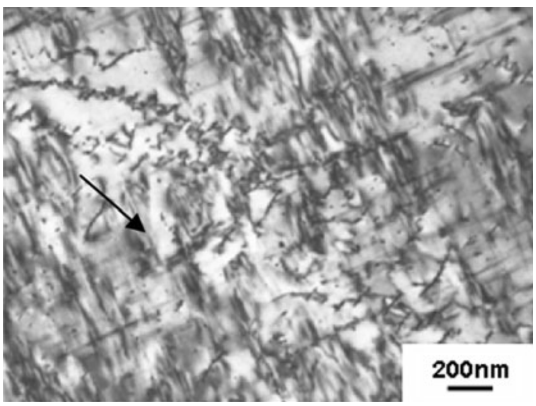

Fig. 11 Stress contrast and dislocation distribution in the matrix of 2D70 alloy crept at 180 °C for 100 h

constant, b is the Burgers vector, λ is the distance among particles, K is a constant, T is the absolute temperature, and σ_{eff} is the effective stress.

The creep behaviors of alloys have close relations with volume fraction of particle, distance among particles, dislocation jog density, and performance temperature.

The main precipitates for the aged samples are S phase with an average length of 50 nm, and S″ phase. After creeping at 150, 180, and 240 °C for 100 h, the S phase grows to 350, 360, and 480 nm, respectively. The precipitated S″ on aging treatment translates to S, and S tends to coarsen. The solid solute atoms in the supersaturation solid solution precipitate dynamically and further proceed to form fine S and S″ phases. There are obvious interactions

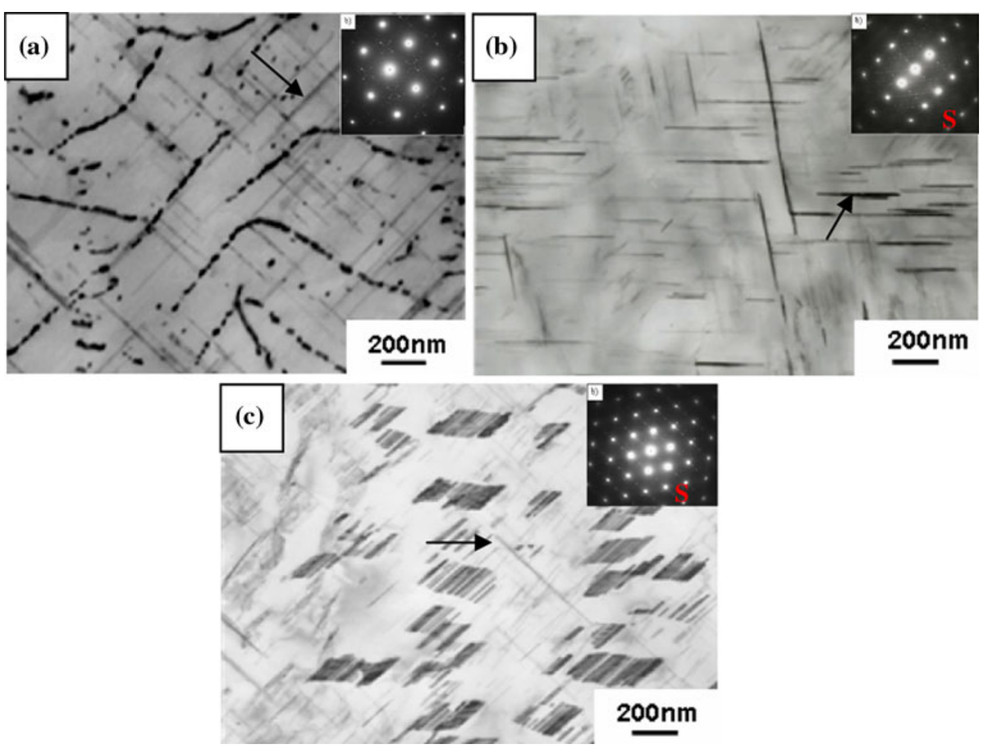

Fig. 12 TEM image and SAED patterns of crept at 240 °C in: **a** [100] zone, **b** [112] zone, and **c** [110] zone

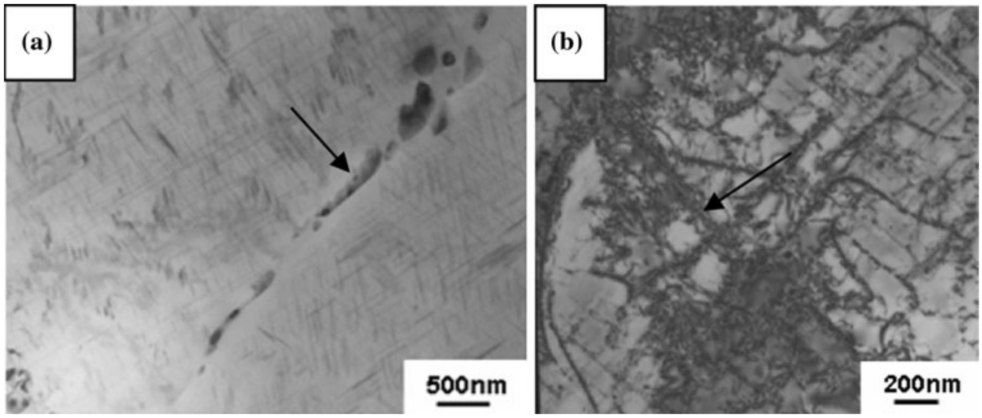

Fig. 13 Precipitates on grain boundary (**a**) and interaction between the precipitates in [100] zones and dislocations (**b**)

between dislocations and precipitates, having effective pinning to dislocation and impeding dislocation movement. A great number of dislocations tangled around the precipitated nanometer particles, such as Al_9FeNi, Al_7Cu_4Ni and Al_7Cu_2Fe, within the grain are observed after creep, which improve the creep behaviors of 2D70 alloy.

The mechanisms for the improved creep property in 2D70 alloy investigated are concluded as follows:

(1) A great number of dislocations generate during creep, and obvious dislocation stacking exists around nano-precipitates, such as $A1_9FeNi$, Al_7Cu_4Ni, and Al_7Cu_2Fe, which help in locking dislocation movement and enhancing the creep resistance.
(2) The precipitated S phase prefers to aggregate on dislocations and interacts with dislocations. The precipitates have effective pinning to dislocation and impede dislocation movement, leading to an increased creep resistance.
(3) The dislocation lines in the crept samples are flat and parallel to each other. Some of them are parallel to the basal plane, showing that the jog climbing is the principal climb mode during creep.

Conclusion

The microstructural evolution of a double solid solution treated Al–Cu–Mg–Fe–Ni alloy was investigated in this study. The conclusions are summarized as follows:

(1) The crept ultimate strength of a double solid solution treated Al–Cu–Mg–Fe–Ni alloy decreases from 312 MPa at 150 °C to 117 MPa at 240 °C.
(2) The precipitates of aged Al–Cu–Mg–Fe–Ni alloy are consisted of S phase and S″ phase, in which the average length of S is 50 nm. After creep, the precipitated S formed at aging treatment coarsens significantly from 350 to 480 nm when creep temperature increases from 150 to 240 °C for 100 h and the precipitated S″ phase translates to S phase simultaneously. The fine S and S″ phases that are further formed resulted from the dynamic precipitation of solid solute atoms from supersaturated solution. These phases act as pinning dislocation and impeding dislocations movement.
(3) There are a great number of dislocations stacking around the nano-Al_9FeNi intermetallic and dislocation array distributed along ⟨022⟩ direction, which are beneficial for S phase pinning and impeding dislocation movement. In addition, there are obvious interactions between dislocations and precipitates, leading to enhanced mechanical properties at elevated temperatures.

Acknowledgement The authors acknowledge the financial support from Heilongjiang Province Science Fund for the Distinguished Young Scholars under program JC201013.

References

1. Novy F, Janecek M, Kral R (2009) J Alloy Compd 487:146
2. Bergsma SC, Li X (1996) J Mater Eng Perform 5:100
3. Wang J, Yi D, Su X, Yin F (2008) Mater Charact 59:965
4. Ber LB (2000) Mater Sci Eng A 280:83
5. Bardi F, Cabibbo M, Spigarelli S (2002) Mater Sci Eng 334:87
6. Yu K, Li W, Li S, Zhao J (2004) Mater Sci Eng A 368:88
7. Majimel J, Molenat G, Casanove MJ (2002) Scripta Mater 46:113
8. Roldan M, Sifferlent R (1972) Acta Metall 20:829
9. Singer R, Blum WZ (1977) Metallkde 68:328
10. Wang G-j, Xiong B-q, Zhang Y-a, Li Z-h, Li P-y (2009) Int J Miner Metall Mater 16:427
11. Djakovic A, Basoalto HC, Dyson BF, McLean M (2005) Metalurgija 11:257